Optik - International Journal for Light and Electron Optics 212 (2020) 164681

Contents lists available at ScienceDirect

Optik

journal homepage: www.elsevier.com/locate/ijleo

Impact of Cd-addition upon optical properties and dispersion parameters of thermally evaporated $Cd_xZn_{1-x}Se$ films: Discussions on bandgap engineering, conduction and valence band positions

Ahmed Saeed Hassanien[a,b,*], R. Neffati[c,d], K.A. Aly[e,f]

[a] Engineering Mathematical and Physics Dept., Faculty of Engineering at Shoubra-Cairo, 11629, Benha University, Egypt
[b] Department of Physics, Faculty of Science and Humanities in Afif, 11921, Shaqra University, Saudi Arabia
[c] Department of Physic, Faculty of Science, King Khalid University, P.O. Box 9004, Abha, Saudi Arabia
[d] IPEIN, Carthage University, Campus Universitaire Merazka, 8000 Nabeul, Tunisia
[e] Department of Physics, Faculty of Science and Arts Khulais, University of Jeddah, Khulais, Saudi Arabia
[f] Department of Physics, Faculty of Science, Al-Azhar University, Assiut branch, Assiut, 71524, Egypt

ARTICLE INFO

Keywords:
ZnSe-CdSe films
Thermal evaporation technique
Optical properties
Swanepoel's envelope method
Wemple DiDomenico model
Chemical bond approach model

ABSTRACT

This research was devoted to study the impact of replacing Cd on the account of Zn of ternary chalcogenide $Cd_xZe_{1-x}Se$ ($0 \leq \times \leq 1.0$) films. In addition, to study the optical characteristics of these films. Physical vapor deposition technique under vacuum about 10^{-5} pa has been used to prepare the film samples. Film thicknesses and the deposition rate were fixed at about 750 nm and 10 nm/S, respectively. The deposited films have been annealed in vacuum at 500 °C for 2 hours. X-ray diffraction technique showed that annealing film samples have a polycrystalline nature of face centered cubic structure. The average crystallite size, D of annealed $Cd_xZn_{1-x}Se$ films proves that these films possess the nanocrystalline structure, where their D-values increase from 26.38 nm to 39.24 nm. Energy dispersion of X-ray spectroscopy technique was used to analyze the elemental composition of films. Optical properties and parameters were deduced from the transmittance and reflectance spectra using spectrophotometric measurements in the range 300 nm - 2500 *n*m. The single oscillator model of Wemple DiDomenico was utilized also to discuss the dispersion energies of Cd-Zn-Se films. Optical constants (n and k) and the absorption coefficient have been extensively studied. Optical bandgap and band-tail energies, as well as some nonlinear optical parameters were discussed. The chemical bond approach model was used to study the cohesive energy and average coordination number of the films. The position of the valence and conduction bands as well as the CB- and VB- potential values have been studied and discussed.

- Polycrystalline films of $Cd_xZn_{1-x}Se$ matrix have been prepared by thermal evaporation technique.
- Dispersion energies values and Sellmeier parameters of films were estimated and studied.
- E_g decreased from 2.663 to 1.677 eV while E_e increased from 0.104 to 0.153 eV, as Cd increased.

* Corresponding author at: Engineering Mathematics and Physics Department, Faculty of Engineering at Shoubra - Cairo, 11629, Benha University, Egypt.
E-mail addresses: a.s.hassanien@gmail.com, ahmed.hassanien@feng.bu.edu.eg (A.S. Hassanien).

https://doi.org/10.1016/j.ijleo.2020.164681
Received 13 December 2019; Received in revised form 25 February 2020; Accepted 31 March 2020

- Chemical bond approach model was used to study bond distributions and cohesive energy values.
- Conduction and Valence Band Positions of CdZnSe system were deduced and discussed.

1. Introduction

Recently, the use of n-type semiconducting materials of II-VI group has increased dramatically and the synthesis of their compositions has grown also exponentially. This is because of their scientific importance and their many potential applications, especially in the electronic and optoelectronic devices and applications. The binary, ternary and quaternary alloys of these materials have attracted the attention of many scientists and researchers, due to the possibility of controlling, tuning and tailoring of their physical, optical and electrical properties [1–4]. Therefore, many of the researchers have allocated their efforts for the synthesis these materials in their bulk form or films as well as studying their physical characterstics. Among these crucial materials, the chalcogenide systems like CdTe, CdSe, CdS, ZnTe, ZnSe, ZnS, Cd-Se-S, Cd-Se-Te, Cd-Zn-S, Cd-Zn-Se, … etc., due to the possibility of engineering their band-gap energy. Where, the values of the band-gap energy of these alloys/compositions are strongly dependent upon their elemental constituents and the proportion of each component [5–8]. These chalcogenide binary and ternary systems are characterized by some unique and distinguish properties such as they are environmentally friendly, slowly react with atmospheric moisture, infrared optical material and have many other distinctive properties [9–11]. On the other side, they are toxic materials, like the other selenides, therefore it must be avoided or inhaled, generally it must careful when be at using them [12–14].

Moreover, the ternary chalcogenide Cd-Zn-Se alloys and compositions have utilized in several and various potential photo-conductive/optoelectronic devices and applications like transistors, optical waveguides, photo electrodes, light-emitting diodes, electro-photography, optically controlled switches, sensors, thin film transistors, laser screens, radiation detectors, laser devices, and solar cells [15–19]. Where, these systems have great electro-optical benefits, where their energy gap can be modulated and engineered, as well as they have significant absorption coefficients and have a strong binding energy between their elements [1,8]. Furthermore, Chalocogenides Cd-Zn-Se systems have direct band-gap energy, E_g and its value lies between Eg of CdSe and ZnSe depending on many parameters. There parameters can change/control the band gap: (i) the used deposition technique, (ii) the used substrate, (iii) the applied experimental preparative conditions (which differ from technique to another) and (iv) the fractional ratios of the compositional elements. The most important parameter is the ratio of Cd and Zn in the Cd-Zn-Se matrix. Furthermore, CdSe and ZnSe compounds can be crystallized in the hexagonal and the cubic (face centered cubic, FCC) structure according to the used preparation technique and the applied preparative conditions [1,8,15].

On the other side, cadmium zinc selenide films can be deposited by using several synthesis techniques, such as chemical bath deposition [2,14], solution growth technique [15], vapor phase deposition [13], spray pyrolysis method [14], ionic layer adsorption and reaction (SILAR) method [18], molecular beam epitaxy [19,20], electron beam pumping [21,22], electron beam evaporation [23], electro deposition [24], pulsed laser deposition [25], and the thermal evaporation [1,3,8,26]. Thermal evaporation, or physical vacuum deposition technique is considered as the most attracting, reliable and convenient technique to deposit the Cd-Zn-Se films. This is due to its relatively low cost, easy substrate loading and high deposition rate, its remarkable ability to obtain good quality films of homogenous thickness. Furthermore, it can control in the deposition conditions of films, such as the deposition rate, film thickness, the morphology of the film surface and its structural state [1,3,8]. Consequently, and because of these mentioned important and crucial advantages, this deposition technique is widely used in the preparation of thin films in compared with the other methods, especially those used in the micro fabrication devices and manufacture of the opto-electronic industries.

In the present research work, the authors will allocate their efforts to study of ternary $Cd_xZn_{1-x}Se$ systems and their films, as a result of their technological and industrial importance. Where, these systems are characterized by the ability to control the band-gap energy according to the required usage via determining the proportions of the constituent elements of the composition. These ternary Cd-Zn-Se compositions are preferable in compared with the binary CdSe or ZnSe compositions, where they more stable and have more absorbance efficiency in the visible region. In addition, they have a wide band-gap covers a considerable large distance from the electromagnetic spectrum, therefore they can be used in the solar cell fabrications.

The aim of the present work is to synthesis thermally evaporated film samples of high-quality nature and of homogeneous thickness from the ternary chalcogenide $Cd_xZn_{1-x}Se$, (x = 0.2, 0.4, 0.6, 0.8 and 1.00 at. %). In addition, to study their optical properties and determination of some optical parameters and their dependence upon the fractional compositional elements of each composition. The authors aim also to deduce the film thickness and the refractive index of the prepared film samples using the Swanepoel's envelope method employing the transmittance spectra only. The single oscillator model of Wemple Di-Domenico was utilized to evaluate the refractive-index dispersion and some other related parameters like the average energy-gap, E_o and the dispersion-energy, E_d values. This work is also aimed to estimate practically some other crucial optical parameters such as the absorption coefficient, extinction coefficient and the non-linear optical constants. As well as, to discuss and study the effect changing the compositional elements on the studied optical characterization of the prepared cadmium zinc selenide matrix.

2. Materials and experimental procedures

Films samples of the chalcogenide $Cd_xZn_{1-x}Se$ matrix (x = 0.2, 0.4, 0.6, 0.8 and 1.0) have been prepared from fine powders of cadmium, zinc and selenium elements. The solid solution reaction method was used to obtain this ternary matrix. Stoichiometric quantities of the elemental powders of Cd, Zn and Se have been mixed together. The atomic weights of the mixed powders were 112.4, 65.38 and 78.96 gm/mol, respectively. They have been purchased from Kock-Light Limited, Haverhill, England and they have a high purity degree (5 N). The appropriate amounts of the three elements were weighed using high sensitivity digital balance

(Sartorius). Then they enclosed within silica ampules and then sealed under vacuum of about 10^{-3}. These sealed silica ampules were placed within a shaker electric oven and the temperature of the oven was raised up gradually by the rate 300 °C/hr till the furnace reached to 500 C and then the temperature of the oven was fixed for one hour. After this temperature, the furnace degree was raised up again, but with a slower rate, 180 °C/hr till the temperature became 800 °C. Noting that, the furnace temperature was fixed for 2 hours at 600 °C and 700 °C while at 800 °C it was fixed for 4 hours. Keeping the temperature of the silica ampoules constant within the furnace with the continuous shaking have been done to guarantee the good homogeneity of the composition of each silica ampoule. Silica tubes have been removed from the electric oven and then suddenly quenched in an ice-water mixture (Melt quenching process). Then the silica ampules have been broken and the ingots bulk composition of each ampule was obtained. A small portion of the obtained bulk composition was used to prepare the film samples.

The thermal evaporation technique was utilized to synthesize the film sample by using Denton-Vacuum coating unit (DV model 502 A) at a pressure ≈ 10^{-5} Pa. The film thickness and the deposition rate were fixed around ≈ 750 nm and 10 nm/S, respectively for all prepared samples. They have been controlled using a quartz crystal monitor. The deposition process has been carried out on pre-cleaned glass substrates. Where, these glass substrates were previously cleaned with a mixture of hydrochloric and nitric acids, then rinsed with a doubly distilled water, then dried in an autoclave oven and then they were ultrasonically cleaned, too. To deposit the film sample, a small portion of the Cd-Zn-Se-ingots were placed in the molybdenum boat (source of the evaporation coating unit) and the evaporation process was carried out. Taking into consideration that the glass substrates have been fixed upon a rotary disc within the coating unit during the evaporation process to obtain film samples of consistent thickness.

The deposited films have been annealed in the vacuum at 500 °C for 2 hours to get crystalline film samples. The film thickness of annealed samples has been experimentally estimated by using the multiple-beam-Fizeau fringes in reflection technique, MBFFR and then affirmed by Swanepoel's envelope method, SM by using the measured transmittance spectra [27]. The measured and evaluated values of the thickness of films, by using the the MBFFR and SE methods, were listed in Table 1. The error in the measurements of thickness between the two methods does not exceed ± 6 nm.

X-ray diffraction technique was used to examine the amorphous/crystallinity nature of as deposited and annealed film samples. A Philips PW-1710 X-Ray diffractometer of the type 1710 has been used. It has a Ni-Cu filtered of K_α-radiation of wavelength ≈ 1.54184 Å. The compositional elements of the present annealed $Cd_xZn_{1-x}Se$ film samples have been analyzed by using the energy dispersive X-ray analysis (Link analytical EDS). The optical transmittance measurements have been done in the spectral range extended from 300 nm to 2500 nm by using the spectrophotometer. Where a double beam computer-controlled spectrophotometer, Jasco V-630 connected with a Lab Top, was set up. Since, the spectrophotometer has a slit of width about 1 nm, which is very small in comparison with the line width, therefore it was needless for making any corrections for the width of the slit. The separated distance between two successive interference maxima (T_M) and minima (T_m) was considered to be the width of the spectral line [28]. Swanepoel's envelope analysis method has been employed to determine the optical characterization of the $Cd_xZn_{1-x}Se$ films by using their transmittance measurements [27,28]. Origin Lab software program of version 2018 has been employed to make the present calculations.

3. Results and discussion

3.1. XRD Structural analysis and EDX confirmation

The X-ray diffractometer had been operated at an electric current 35 mA and voltage 40 kV. As well as, the used wavelength was 0.154184 nm and the applied energy was 8.042 keV [6,29]. This strong energy is enough to examine the prepared CdZnSe thin films. A continuous scanning was applied at a slower scan rate (1°/min) and a smaller time constant equals 1 s to detect any possible diffraction line [30,31]. Fig. (1) shows the X-ray diffractograms of the present ternary chalcogenide $Cd_xZn_{1-x}Se$ film samples (x = 0.2, 0.4, 0.6, 0.8 and 1.0). It was observed that before the annealing process of films, all films have the amorphous nature. But after the annealing process of film samples, X-ray diffraction patterns affirmed that they became to have the polycrystalline nature. This crystallinity nature of Cd-Zn-Se films depicts three diffraction peaks of Miller indices (111), (220) and (311) at the diffraction Bragg angles 27.477°, 45.637 ° and 54.098 ° for the annealed ZnSe film sample. Similar results have been obtained in the previous literature [32–34].

Table 1
The film thickness as obtained by MBFFR and SE methods and the crystallite size, D, as well as the selected and measured compositional element ratios of $Cd_xZn_{1-x}Se$ film samples.

Composition	Film thickness (nm)		Crystallite size (nm)	Calculated values %			Measured Values %		
	By MBFFR	By SE		Cd	Zn	Se	Cd	Zn	Se
ZnSe	778	783	26.38	0.00	50.00	50.00	0.00	50.06	49.94
$Cd_{0.2}Zn_{0.8}Se$	756	750	27.21	10.00	40.00	50.00	9.97	39.94	50.09
$Cd_{0.4}Zn_{0.6}Se$	740	734	31.08	20.00	30.00	50.00	19.95	29.91	50.11
$Cd_{0.6}Zn_{0.4}Se$	758	764	32.94	30.00	20.00	50.00	30.03	20.06	49.91
$Cd_{0.8}Zn_{0.2}Se$	731	725	34.79	40.00	10.00	50.00	40.07	9.86	50.07
CdSe	729	725	39.24	50.00	0.00	50.00	49.95	0.00	50.05

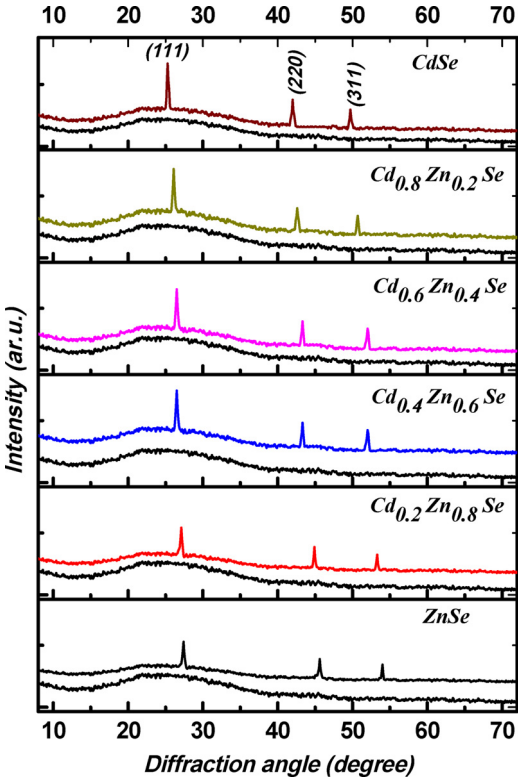

Fig. 1. XRD-patterns of as-deposited and annealed $Cd_xZn_{1-x}Se$ films. The amorphous nature belongs to as-deposited films, while the polycrystalline phase has been obtained after annealing.

These three diffraction lines were observed to be shifted towards the smaller diffraction angles. This shift increased with increasing the Cd-content within the study matrix. For the CdSe film sample, the same three diffraction peaks appeared at the angles 25.375°, 42.044° and 49.741°. No other diffraction lines were detected in all samples. This indicates that there are no any other phases were formed. These diffraction lines at these diffraction angles affirm that the films have crystallized in the cubic structure (face centered cubic).

These results are fully consistent with X-ray diffraction JCPDS-ICDD database-cards (Joint Committee on Powder Diffraction Standards- International Center for Diffraction Data) of database-cards of the following numbers (JCPDS: 80-0021 and JCPDS: 88–2345) for ZnSe and (PDF 03-065-2891, PDF 03-065-2891, JCPDS: 19-0191 and JCPDS: 77-2307) for CdSe and they have displayed the cubic-zinc-blende-structure type, where it is well known that both ZnSe and CdSe crystallize as either cubic or hexagonal according to the deposition conditions [1,3].

It was observed also the preferred crystallographic orientation of all samples is along the major diffraction line (111). It is worthy to note also that the obtained the intensity of the three diffraction lines increased with increasing the Cd-content within the studied $Cd_xZn_{1-x}Se$ network. This indicates that the presence of more Cd-element leads to increase the crystallinity nature more than Zn-element. The observation of the existence of the diffraction line (111), which has the highest peak for all the film samples of Cd-Zn-Se network confirms the formation of the Cd-Zn-Se alloys. These results are in good matching with previous works in literature [1,3,8,35–38].

Moreover, based on the shown XRD patterns, Fig. (1) and using the well-known equation of Scherrer $D = k \lambda / (\beta \cos \theta_{(h,k,l)}$ [13,30], it can estimate the crystallite size of the polycrystalline Cd-Zn-Se film samples. The Scherrer formula relates between the crystallite size, D and the Bragg's diffraction angles, $\theta_{(h,k,l)}$. Therefore, and to calculate the crystallite size of the film samples, the following procedure was carried out: the observed X-ray diffractograms were refined by removing the instrumental broadening. Where, the net resultant broadening of the film sample itself, β can be evaluated from the observed broadening (B) and the instrumental broadening (b) (due to the used apparatus). Thereby, $\beta = B - b$, and its value can be obtained from the full width at half maximum (FWHM) of the X-ray diffractograms. Moreover, the constant k that is mentioned in the above Scherrer Eq. is called the shape factor and equals 0.94.

Hence, the average crystallite size values of the film samples can be determined from the three diffraction lines and then the average D-values were recorded in Table 1. It is worth noticing that the estimated D-average values prove that the annealed $Cd_xZn_{1-x}Se$ films possess the nanocrystalline structure, where their D-values increase from 26.38 nm to 39.24 nm as the Cd-ratio increased. The increase of the crystallite size of samples is owing to the formation of crystalline cluster agglomerations and the coalescence of smaller crystals with each other because of annealing process and the addition of more Cd to the host lattice [7,13].

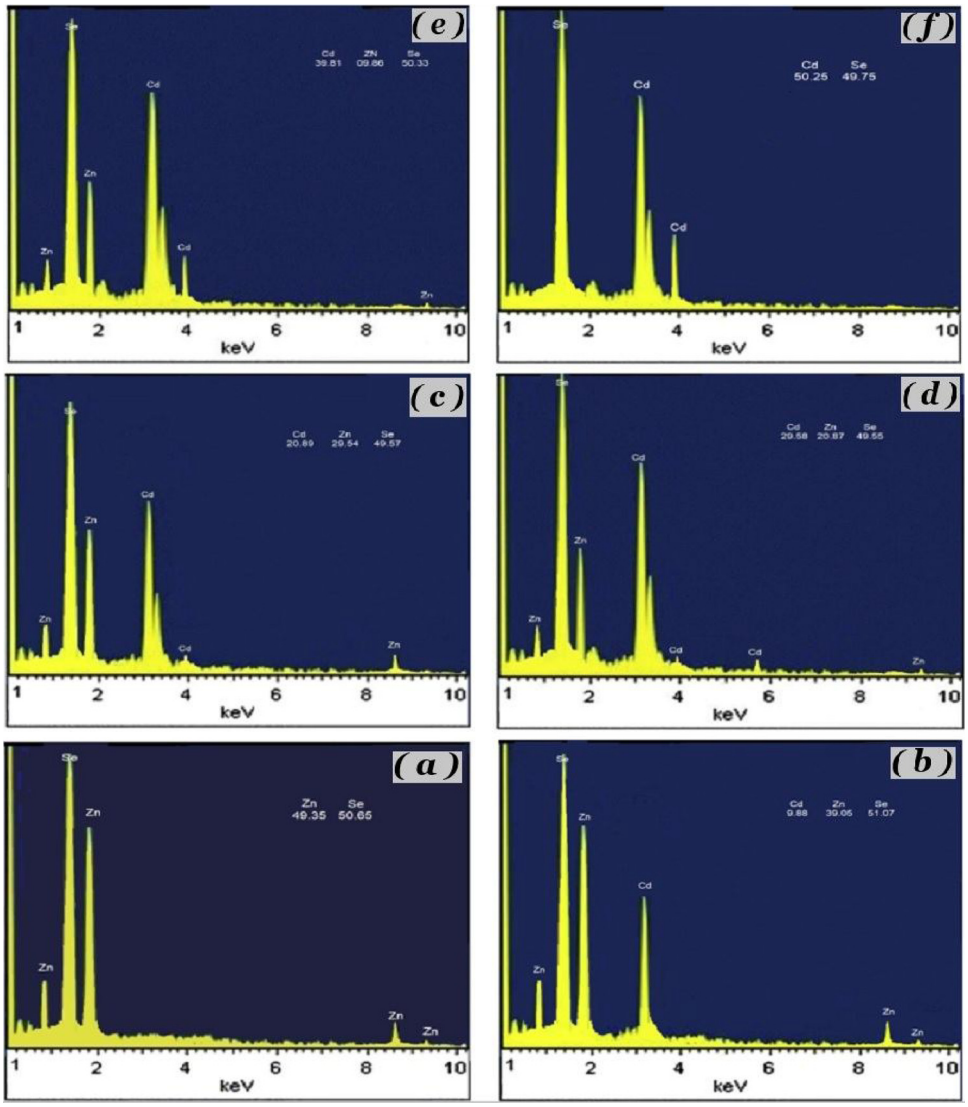

Fig. 2. EDX images of the six polycrystalline annealed Cd-Zn-Se samples: (a) ZnSe, (b) $Cd_{0.2}Zn_{0.8}Se$, (c) $Cd_{0.4}Zn_{0.6}Se$, (d) $Cd_{0.6}Zn_{0.4}Se$, (e) $Cd_{0.8}Zn_{0.2}Se$ and (f) CdSe.

On the other hand, the compositional elements of the ternary $Cd_xZn_{1-x}Se$ were analyzed using EDX technique. It was found that there is a good consistent between the calculated and the obtained measured values by EDX-technique. Fig. (2) shows the EDX spectra of the six samples of Cd-Zn-Se films. This figure displays also that the exhibited peaks are in accordance with the Zn, Cd, and Se atomic-ratio values, i.e. they are in good matching with the selected ratios. Hence, the current Cd-Zn-Se films are stoichiometric compositions. Furthermore, Table 1 reports the good matching between the calculated fraction elemental ratios and those estimated from the energy-dispersive-X-ray spectroscopy, EDX measurements.

3.2. Optical spectra studies

The optical transmittance, T indicates to the ability of electromagnetic waves to penetrate the material films. The importance of the optical transmittance of light waves through materials is attributed to their usages in the potential applications like optical fibers, the optoelectronic devices, and the other photonic applications. Figs. (3 -a, b and 4) depict the transmittance (T) spectra of the annealed film samples of the ternary Cd-Zn-Se matrix. These spectra, as observed are basically interference fringes of maxima and minima patterns alternate between about 65 % and 85 % for the transmittance.

Moreover, Fig. (5) illustrate the reflectance spectra and its behavior versus the wavelength of incident photon (λ). It should be noted that this figure also shows that the reflectance spectra (R) are interference fringes just like the transmittance spectra (T), too. Furthermore, the maxima of T-spectra meet the minima of R-spectra and vice versa, where the sum of both T and R intensities at any

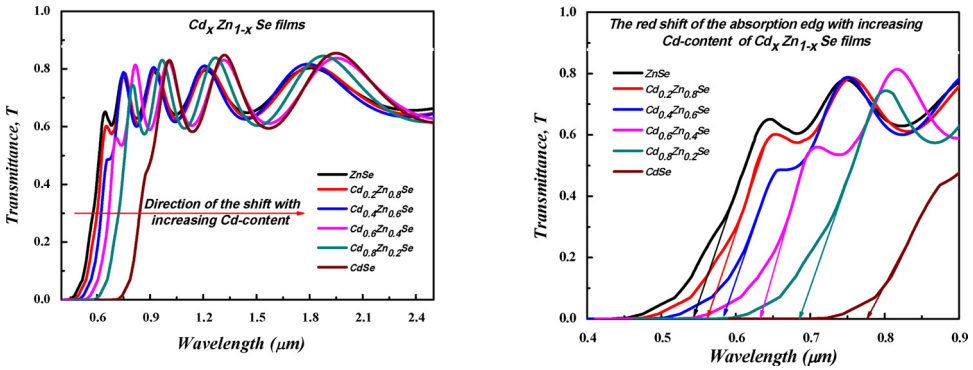

Fig. 3. Transmittance, T spectra and the Redshift of the absorption edge of $Cd_xZn_{1-x}Se$ ($0 \leq x \leq 1$) films.

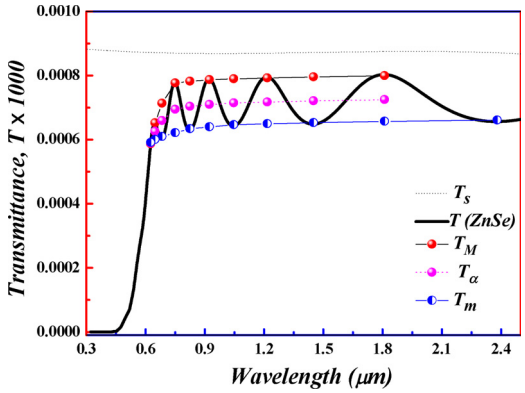

Fig. 4. The transmittance spectra of annealed ZnSe film sample as a typical sample for the annealed crystalline $Cd_xZn_{1-x}Se$ films, where T_s is the glass-substrate transmittance, T_M, T_m and T_a are the maximum, the minimum and the average experimental values of the transmittance.

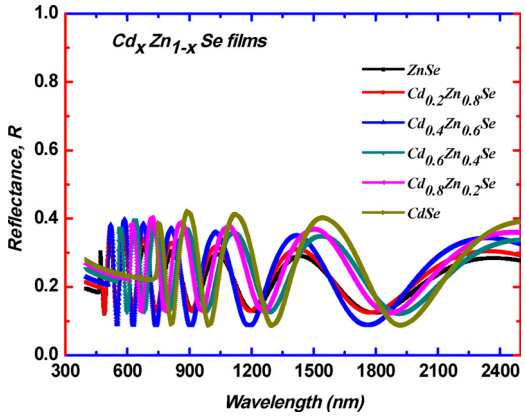

Fig. 5. The reflection spectra of the crystalline annealed Cd-Zn-Se film samples.

given wavelength is always less than 100 percent. Fig. (3-a) and (b) of T-spectra also illustrate that no interference fringes, IF near the absorption edge, but these IF do not begin to appear until after a wavelength of about 500-600 nm. The appearing of these IF in both T and R spectra by these high intensities emphasizes the good quality and the regularity of the film thickness of the present films.

Furthermore, Fig. (3)-(a) and (b) show that after the absorption edge, the intensity of T-spectra is dramatically increased. As well as, the absorption edge itself shifted towards the higher wavelengths, as shown in Fig. (3 -b), when the Cd-concentration was increased from 0.00 to 1.00 in the Cd-Zn-Se matrix. This figure depicts also that this absorption edge is redshifted from about 460 nm to about 740 nm, i.e. a redshift of the band-gap is occurring as Cd-content increased.

It is worth mentioning that, the occurrence of this redshift of the absorption edge or the band-gap position can be interpreted in the light of the improvement of the crystallization process of films when Cd-content was increased and with the influences of the quantum confinement and the removing of the residual thermal stresses due to the annealing process of samples. Moreover, Fig. (4)

depicts the transmittance spectra of the sample of ZnSe-film (i.e. Cd-content is zero) as a typical curve. Fig. (4) illustrates also more details about the T-spectra of the studied Cd-Zn-Se films, where it shows how the envelope method as suggested by Swanepoel can be employed [36–38]. As shown in the figure, T_M, T_m and T_s are the maximum, the minimum and the substrate transmittances, respectively.

4. Evaluation of the film thickness and refractive index

The film thickness and refractive index of the annealed films of Cd-Zn-Se network can be estimated by using the envelope method as assumed by Swanepoel, EMS. Depending upon Manifacier and his co-authors' idea [36] and based on EMS [37], the first approximation of the refractive index value, n_1 of weak and medium absorptions can be determined by this formula [3,37,38]:

$$n_1^2 = [N + (N^2 - S^2)^{1/2}] \quad (1)$$

where, N is given as:

$$N = 2S\left(\frac{T_M - T_m}{T_M.\ T_m}\right) + \left(\frac{S^2 + 1}{2}\right) \quad (2)$$

where, T_M is the maximum and T_m is minimum transmittances at a certain wavelength, which have been generated and computed by OriginLab version 2018 software and S is the substrate refractive index, which is given as follows [37–39]:

$$S = \frac{1}{T_S} + \left(\frac{1}{T_S^2} - 1\right)^{1/2} \quad (3)$$

where, T_s is the transmittance of the glass substrate. Consequently and from Eqn. (1), n_1-values were determined and recorded in Table 2. Depending upon the calculated values of n_1 and by substituting with n_1-values in the Eqn. of the interference fringes, which is given by this relation [37,38]:

$$2nd = m_o\,\lambda \quad (4)$$

where, the order number, m_o is an integer number (0, 1, 2, 3 …) for the maxima while for minima it is a half integer number (1/2, 3/2, 5/2 …). For two successive maxima or two successive minima and have the refractive indices n_{c1}, and, n_{c2}, the first approximation value of the film thickness, d_1 is given as follows [40]:

$$d_1 = \lambda_1.\lambda_2 \,/\, 2(n_{c2}\,\lambda_1 - n_{c1}\,\lambda_2) \quad (5)$$

where, ***λ_1 and λ_2*** are the wavelengths of the two selected successive maxima or minima IF.

Thereby, the film thickness could be determined. The estimated values of the film thickness, d of the annealed polycrystalline Cd-ZnSe films were listed in Table 2, in addition to the estimated n_1-values and d_1-values, too. Noting that, there are some calculated values have been excluded because they were too far from the other values. By knowing the d-values and their average values, $\bar{d}_1$, one can calculate m_o-values for all maxima and minima IF using Eqn. (4). The thickness of the film was greatly increased by using the exact values of m_o, either they integer numbers or half integer numbers, relating to the end point, as shown in Fig. (2), consequently, the final thickness values (d_2) can be estimated. It should mention that by using the current procedure, the calculated d_2-value of films does not have a considerable dispersion. Where the error in the film thickness does not exceed ± 1 %, as it was affirmed from multiple-beam-Fizeau fringes in reflection experiment, as reported in Table 1. Depending upon the estimated exact m_o- and d_2-values (noting that $d = d_2$). Thus, Eqn. (4) can be solved and the refractive index, n can be calculated at every wavelength, λ and then tabulated in Table 2, too.

Further, the number of the first order, m1 and the thickness of films, d-values can be easily derived based on a simple graph and using Eqn. (1). Hence and starting with the highest wavelengths at the position of the occurrence of the maxima and minima IF, and re-arranging Eqn. (4) to get the following formula [38,41]:

$$\frac{l}{2} = 2d\left(\frac{n}{\lambda}\right) - m_1 \quad (6)$$

where, d, n, λ and m_1 are the film thickness, the estimated refractive index, the wavelength and the value of the first order, respectively, noting that m_1- values are integers for maxima and half integer for minima IF. As obvious, the last equation can be represented graphically, where (l/2) is plotted on the vertical axis and (n/λ) is plotted on x-axis, as shown in Fig. (6). Thereby, the relationship between (l/2) and (n/λ) will be a linear relationship and the slope of each line is the twice the value of d-value, while the intercept of y-axis is the value of m_1. Therefore, anyone can obtain the d- and m_1-values. The calculated values of both n and m_1 were also reported in Table 2. Furthermore, the empirical equations describing these obtained straight lines have been developed and given as follows:

For ZnSe, $l/2 = (1.566\ n/\lambda) - 2.0$, for $Cd_{0.20}Zn_{0.80}Se$, $l/2 = (1.506\ n/\lambda) - 2.0$

for $Cd_{0.40}Zn_{0.60}Se$, $l/2 = (1.460\ n/\lambda) - 1.5$, for $Cd_{0.60}Zn_{0.40}Se$, $l/2 = (1.534\ n/\lambda) - 2.0$

Table 2
The estimated optical parameter values, the film thickness and the refractive indices of the annealed polycrystalline films of Cd-Zn-Se matrix using the envelope method of Swanepoel.

λ	T_M	T_m	T_s	n_1	d_1(nm)	m	m_{exa}	d_2(nm)	n_2
1440	0.855	0.698	0.872	2.303	–	2.543	2.5	782	2.299
1206	0.856	0.695	0.870	2.322	767	3.061	3.0	779	2.310
1037	0.856	0.693	0.869	2.332	772	3.576	3.5	778	2.318
914	0.855	0.689	0.869	2.345	790	4.079	4.0	780	2.335
817	0.856	0.685	0.869	2.357	783	4.587	4.5	780	2.348
742	0.856	0.679	0.870	2.373	798	5.085	5.0	782	2.369
679	0.854	0.674	0.871	2.381	811	5.575	5.5	784	2.385
628	0.851	0.668	0.872	2.393	821	6.059	6.0	787	2.406
ZnSe $\bar{d}_1 = 792\,nm$, $\delta 1 = 20\,nm$ (2.5 %), $\bar{d}_2 = 783$, $\delta 2 = 3\,nm$ (0.38 %)									
1426	0.862	0.679	0.872	2.380	—	2.654	2.5	749	2.377
1196	0.860	0.675	0.869	2.399	743	3.189	3,0	748	2.392
1030	0.859	0.674	0.869	2.402	766	3.708	3.5	750	2.403
908	0.859	0.666	0.869	2.428	730	4.252	4.0	748	2.421
812	0.860	0.662	0.869	2.444	746	4.785	4.5	748	2.436
738	0.860	0.656	0.870	2.460	772	5.300	5.0	750	2.460
677	0.860	0.648	0.871	2.485	742	5.836	5.5	749	2.482
627	0.862	0.641	0.872	2.510	752	6.365	6.0	749	2.508
584	0.862	0.634	0.873	2.532	753	6.892	6.5	750	2.531
$Cd_{0.2}Zn_{0.8}Se$ $\bar{d}_1 = 782\,nm$, $\delta 1 = 14\,nm$ (1.7 %), $\bar{d}_2 = 750$, $\delta 2 = 3\,nm$ (0.40 %)									
1419	0.839	0.650	0.871	2.431	—	2.539	2.5	730	2.417
1191	0.836	0.648	0.869	2.441	743	3.038	3.0	732	2.434
1026	0.836	0.643	0.869	2.462	716	3.556	3.5	729	2.446
906	0.835	0.640	0.869	2.471	762	4.042	4.0	733	2.469
811	0.836	0.635	0.869	2.490	730	4.550	4.5	733	2.486
738	0.836	0.628	0.870	2.513	745	5.047	5.0	734	2.514
677	0.837	0.620	0.871	2.537	733	5.553	5.5	734	2.536
629	0.837	0.612	0.872	2.565	757	6.042	6.0	736	2.571
$Cd_{0.4}Zn_{0.6}Se$ $\bar{d}_1 = 765\,nm$, $\delta 1 = 72\,nm$ (9.4 %), $\bar{d}_2 = 734$, $\delta 2 = 6\,nm$ (0.80 %)									
1538	0.855	0.629	0.873	2.534	–	2.557	2.5	759	2.516
1291	0.852	0.626	0.870	2.549	765	3.065	3.0	760	2.535
1112	0.852	0.623	0.869	2.567	750	3.582	3.5	758	2.547
982	0.850	0.617	0.869	2.584	773	4.084	4.0	760	2.571
879	0.850	0.612	0.869	2.603	758	4.596	4.5	760	2.589
800	0.850	0.605	0.869	2.627	776	5.096	5.0	761	2.618
734	0.852	0.598	0.870	2.653	754	5.610	5.5	761	2.642
$Cd_{0.6}Zn_{0.4}Se$ $\bar{d}_1 = 763\,nm$, $\delta 1 = 130\,nm$ (17.1 %), $\bar{d}_2 = 764$, $\delta 2 = 9\,nm$ (1.2 %)									
1496	0.841	0.606	0.872	2.593	—	2.597	2.5	721	2.579
1257	0.839	0.602	0.870	2.614	721	3.116	3.0	721	2.601
1084	0.839	0.598	0.869	2.634	714	3.640	3.5	720	2.617
959	0.837	0.592	0.869	2.656	737	4.148	4.0	722	2.646
860	0.837	0.586	0.869	2.679	723	4.666	4.5	722	2.669
783	0.827	0.578	0.870	2.687	790	5.140	5.0	729	2.700
720	0.805	0.570	0.870	2.673	891	5.560	5.5	741	2.731
$Cd_{0.8}Zn_{0.2}Se$ $\bar{d}_1 = 763\,nm$, $\delta 1 = 69\,nm$ (9.0 %), $\bar{d}_2 = 725$, $\delta 2 = 7\,nm$ (1.0 %)									
1550	0.823	0.593	0.873	2.604	—	2.500	2.5	744	2.622
1302	0.820	0.589	0.870	2.625	743	3.001	3.0	744	2.643
1123	0.819	0.574	0.869	2.688	663	3.562	3.5	731	2.659
993	0.807	0.567	0.869	2.694	782	4.037	4.0	737	2.687
891	0.785	0.551	0.869	2.717	744	4.538	4.5	738	2.713
CdSe $\bar{d}_1 = 763\,nm$, $\delta 1 = 50\,nm$ (6.8 %), $\bar{d}_2 = 725$, $\delta 2 = 5\,nm$ (0.7%)									

for $Cd_{0.80}Zn_{0.20}Se$, $l/2 = (1.458\ n/\lambda) - 1.5$ and for CdSe, $l/2 = (1.478\ n/\lambda) - 2.0$

where the wavelength, λ was expressed in micrometer (μm).

It is worth mentioning that these graphical representations affirm the correctness of the obtained values of the refractive index, n, as well as the values of the parameter (m_1). It is observed also that the obtained d-values from the last figure are well consistent with those values obtained previously from using the envelope method argued by Swanepoel, EMS for the present annealed film samples of Cd-Zn-Se matrix. From the well reading of the calculated data of the refractive index, n which was reported in Table 2, one can easily conclude that n-value of the annealed films of Cd-Zn-Se network has been increased by increasing the Cd-content in the matrix. This result is a natural result, where the cadmium refractive index is greater than that of the selenium and in the same time Cd was increased on the account of Zn, therefore the increment of Cd leads to the increment of the refractive index of the matrix.

Now, by employing the obtained n-values as functions of the reciprocal of the square of the wavelength ($1/\lambda^2$) and substituting in

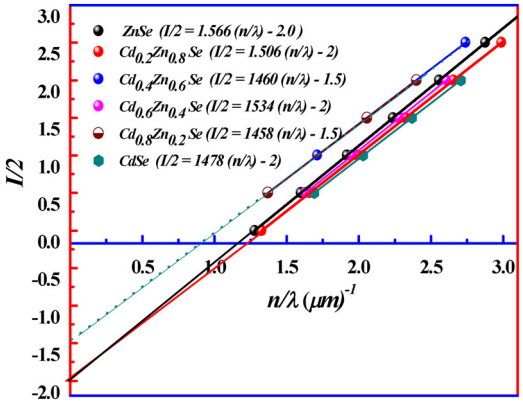

Fig. 6. The representation of (I/2-values) as a function of (n/λ-values) of the polycrystalline annealed films of $Cd_x Zn_{1-x}Se$ system, where ($0.00 \leq x \leq 1.00$) to get d- and m_1-values.

the empirical dispersion Eqn. of Cauchy and making a least square fitting, anyone can easily obtain the following formula of two terms [40,41]:

$$n(\lambda) = a + \frac{b}{\lambda^2} \tag{7}$$

whereas, (a) and (b) are called Cauchy's parameters which can be easily obtained from Fig. (6).

Since the obtained plot is a straight line has a slope and intercept the axes. So, the slope will give the parameter (b) while the intercept part from the y-axis is the value that represent the parameter (a). Hence, and by knowing the values of (a) and (b) anyone can re-substitute into Eqn. (7) and plot another graph links between n-values and (λ) to extend along all the measured spectral range, i.e. 300-2500 nm, as the shown Fig. (7). This figure represents the spectral behavior analysis of the obtained n-values along the studied transmittance spectra included the weak and medium absorption zones for the studied films of Cd-Zn-Se matrix.

In Fig. (7), it should note that the solid and largest symbols are the determined n-values, while the hollow and smallest symbols are those calculated according to the Cauchy dispersion relationship. Fig. (7) illustrates also that along the studied optical spectra the refractive index values are dramatically decreased up to about 1250 nm and after this wavelength they almost become constant values. Besides, the values of the index of refraction, n were found to increase as the ratio of the Cd-content was increased.

These results are in good match with the previous literature [3,36]. Along with, it must also mention that the proportional error in n-values, Δn/n does not overtake that of the measured transmittance, ΔT/T (± 1%). Furthermore, the least square fitting of the n-values of the studied annealed Cd-Zn-Se film samples, as depicted in Fig. (5) via the thin intermittent lines, have been formulated by these empirical Eqns. as follows:

$$\text{For } x = 0.0, \text{ i. e. ZnSe, } n = \frac{55919.40}{\lambda^2} + 2.29$$

$$\text{For } x = 0.2, \text{ i. e. } Cd_{0.20}Zn_{0.80}Se, \; n = \frac{92644.80}{\lambda^2} + 2.50$$

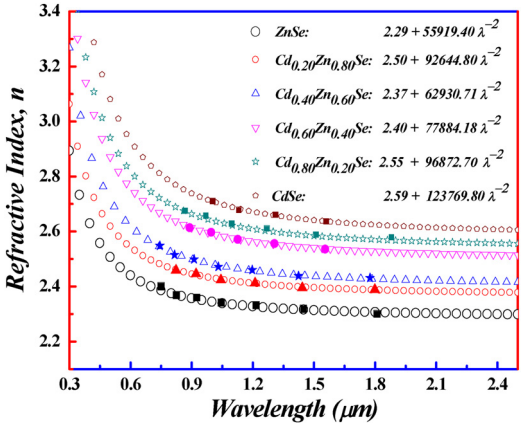

Fig. 7. The normal dispersion spectra of the index of refraction of annealed $Cd_xZn_{1-x}Se$ films where $0 \leq x \leq 1$. The solid and largest symbols are the determined n-values, while the hollow and smallest symbols are observed according to the Cauchy dispersion relationship.

For x= 0.4, i. e. $Cd_{0.40}Zn_{0.60}Se$, $n = \frac{62930.71}{\lambda^2} + 2.37$

For x= 0.6, i. e. $Cd_{0.60}Zn_{0.40}Se$, $n = \frac{778844.18}{\lambda^2} + 2.40$

For x= 0.8, i. e. $Cd_{0.80}Zn_{0.20}Se$, $n = \frac{96872.70}{\lambda^2} + 2.55$

And for x= 1.0, i. e. CdSe, $n = \frac{123769.80}{\lambda^2} + 2.59$

4.1. Single effective oscillator Model studied

The dispersion is an important factor and plays essential roles to select the materials for any potential applications or to be used in the design of optoelectronic devices of the spectral dispersion [3,36]. Hence, this subject must be discussed in details along with, to study the effect of adding the cadmium on the dispersion parameters of the refractive index and the dispersion energies of the polycrystalline films of the Cd-Zn-Se matrix. The best model that can be applied to study these parameters is the Single effective oscillator Model oscillator model suggested by Wemple - Di-Domenico, SEOM-WDD [3,38–44]. This model has successfully studied the effective single oscillator energies (E_o), along with the dispersion or strength energies (E_d) and at the same time, it determines their values by very accurate results. Consequently, and according to Wemple & Di-Domenico dispersion theory, the refractive index, n is related to these energies (E_o and E_d) by the following expression [43,44]:

$$(n^2 - 1) = \frac{E_d E_o}{[E_o^2 - (h\upsilon)^2]} \tag{8}$$

Rearranging this equation to get:

$$(n^2 - 1)^{-1} = \frac{E_o^2 - (h\upsilon)^2}{E_d E_o} = \frac{E_o}{E_d} - \frac{(h\lambda)^2}{E_d E_o} \tag{9}$$

Consequently, this equation can be represented graphically by plotting the index of refraction factor, $[1/(n^2 - 1)]$ against the photon energy squared, $[(h\nu)^2]$, which is graphically illustrated in Fig. (7). Thereby, anyone can get a straight line has a slope equals the $[1/E_d E_o]$ and intercepts the y-axis in a value given by this term (E_o/E_d). Consequently, the energy values of both the effective single oscillator, E_o and the dispersion (strength), E_d can be easily obtained for the annealed film samples of the ternary Cd-Zn-Se network from Fig. (8). The values of both E_o and E_d have determined and listed in Table 3.

It can observe that the effective single oscillator energy values decreased as the ratio of Cd-content was increased. This is probably due to that the effective single oscillator energy, which is occasionally called the mean energy gap, E_o-values are proportional to the optical band-gap-energy value along with it gives some quantitative information about the band structure of materials. The inter-relationship between them is almost E_o equals twice of E_g (i.e. $E_o \approx 2\ E_g$) as suggested by Tanaka [45] and since E_g of CdSe is less than that ZnSe and since Cd increased also on the account of Zn, therefore E_g will decrease and thereby E_o. The interrelationships between the two energies E_o and E_g will be studied in details in a next section.

Based on the evaluated energy parameters of both the effective single oscillator, E_o and the dispersion, E_d, which have been deduced from the employing Wemple-Di-Domenico's model, anyone can deduce also another two parameters for the annealed films of the polycrystalline Cd-Zn-Se network, which are the moments of the optical spectra, donated as M_{-1} and M_{-3}. These two moments are given by these two Eqns. [46,47]:

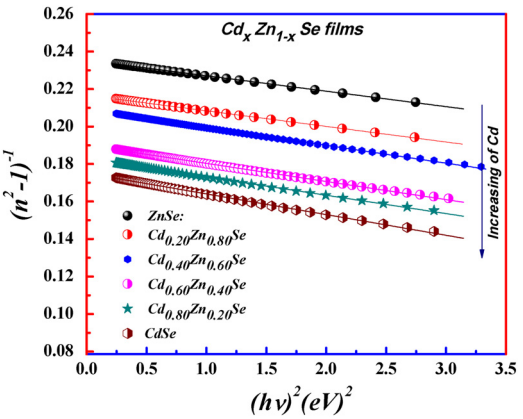

Fig. 8. The index of refraction parameter $[1/(n^2 - 1)]$ Vs $[(h\nu)^2]$ of annealed films of the chalcogenide $Cd_x Zn_{1-x}Se$ matrix, where $(0.00 \le x \le 1.00)$ films.

Table 3
Some essential optical parameters which have been estimated for the annealed polycrystalline films of Cd-Zn-Se matrix.

Estimated optical parameter	Ratio of Cd-content the ternary Cd_xZn_{1-x} Se matrix					
	x = 0.0	x = 0.2	x = 0.4	x = 0.6	x = 0.8	x = 1.0
Dispersion or strength energy, E_d (eV)	21.582	21.903	22.131	22.743	23.481	24.074
Effective single oscillator energy, E_o (eV)	5.414	5.057	4.654	4.427	4.311	4.021
The first moments of the optical spectra, M_{-1}	7.753	7.836	7.884	8.037	8.207	8.347
The second moments of optical spectra, M_{-3}	1.553	1.472	1.370	1.312	1.273	1.192
The dielectric constant of the lattice, ε_L, From Eqn. (12)	4.991	5.346	5.764	6.137	6.447	6.947
The static index of refraction, n_o	2.230	2.312	2.402	2.478	2.539	2.641
The dielectric constant of the lattice, ε_L From Eqn. (13)	5.158	5.392	5.751	6.139	6.449	6.851
The term (N/m*) $\times 10^{52}$ (g·cm)$^{-1}$	4.071	5.096	5.953	7.514	8.436	9.583
The wavelength of the oscillator, λ_o (nm)	230.2	264.3	267.2	281.4	288.8	309.1
The strength of the oscillator, $S_o \times 10^{13}$ (m^2)	7.552	7.154	6.672	6.513	6.554	6.261
Optical band-gap energy, E_g (eV)	2.663	2.560	2.438	2.230	2.025	1.677
The band-tail parameter $\alpha_o \times 10^5$ (cm^{-1})	9.152	8.504	7.861	6.973	6.021	4.695
The ratio, (E_g/E_0)	1.992	1.941	1.930	1.990	2.129	2.469
Band tail width or Urbach's energy, E_e (eV)	0.104	0.113	0.126	0.133	0.137	0.153
Cohesive energy, CE (eV/atom)	4.258	3.517	3.331	3.144	2.958	2.772
Third order nonlinear optical susceptibility, $X^{(3)} \times 10^{-12}$ esu	1.022	1.421	2.061	2.813	3.544	5.149
The nonlinear index of refraction, $n_2 \times 10^{-11}$esu	1.720	2.321	3.242	4.273	5.251	7.344
The plasma frequency, (ω_p) $\times 10^{13}$ Hz	3.701	4.142	4.470	5.026	5.334	5.681

$$E_o^2 = \frac{M_{-1}}{M_{-3}} \; and \; E_d^2 = \frac{M_{-1}^3}{M_{-3}} \tag{10}$$

Solving these two equations with each other, to get:

$$M_{-1} = \frac{E_d}{E_o} \; and \; M_{-3} = \frac{M_{-1}}{E_o^2} \tag{11}$$

Therefore, M_{-1} and M_{-3} can be calculated and then recorded also in Table 3. It is clear that the value of the two moments increased when the Cd-content increased in the annealed film of Cd-Zn-Se network. Furthermore, by knowing the two-dispersion energy values E_d and E_o, which were deduced from Fig. (8), based on the effective oscillator model, anyone can calculate the dielectric constant of the lattice, $\boldsymbol{\varepsilon_L}$ and the static index of refraction, n_o, where they are given as follows [46,47]:

$$\varepsilon_L = 1 + \frac{E_d}{E_o} \; and \; n(0) = \sqrt{1 + \frac{E_d}{E_o}} \tag{12}$$

Hence, the values of both ε_L and n_o have been estimated and tabulated also in Table 3. As obvious, the value of these two optical parameters increased as Cd-content increased.

On the other hand and based on the obtained results of the index of refraction, n, the dielectric constant of the lattice, $\boldsymbol{\varepsilon_L}$ can be obtained again from the plotting of the square value of the index of refraction, n^2 (note that n^2 gives the real dielectric constant, where, $\boldsymbol{n2 = \varepsilon_1}$), against the square of the photon wavelength, (λ^2) according to the following equation [6,48,49]:

$$n^2 = \varepsilon_1 = \varepsilon_L - \left(\frac{e^2}{4\pi^2 c^2 \varepsilon_o}\right)\left(\frac{N}{m^*}\right)\lambda^2 \tag{13}$$

where, the term (N/m*) gives the concentration of free carriers to the effective mass and thereby, the dispersion vibration modes could be determined, too.

Consequently, If the graph is plotted between ($n^2 = \varepsilon_1$) on the vertical axis and (λ^2) on the horizontal axis, then a straight line will be gotten. This line has a slope equals $\left(\frac{e^2}{4\pi^2 c^2 \varepsilon_o}\right)\left(\frac{N}{m^*}\right)$ and intercept the vertical axis at a value equals $\boldsymbol{\varepsilon_L}$. Hence, both the values of the dielectric constant of the lattice, $\boldsymbol{\varepsilon_L}$ and the term (N/m*) could be obtained. Accordingly, the above mentioned have been already implemented and these parameters have been accounted and included also in Table 3. If there is a comparison between the two values of the dielectric constant of the lattice, ε_L obtained from equations (12) and (13), anyone will find that there is a good matching between the two values, and if there is disagreement, it does not exceed a decimal fraction of one thousandth, due to calculations and the approximation. This indicates the validity and accuracy of the obtained results.

Moreover, it can observe from Fig. (7) that the index of refraction, n has a normal dispersion behavior, where it has large values in the region of higher frequencies and has dramatically decreased up at 1250-1300 nm and then it seem to become almost constant for higher wavelengths, i.e. after 1300 nm. This normal behavior is a result of the fact that higher frequency regions are characterized by its high ability to absorb light waves, thereby the speed of light decreases through which, this will in turn increases n-values. Further, the index of refraction became constant due to the speed of light waves become faster, which in turn led to decreases n-values. On the hand, it can see also that the estimated values of the term (N/m*), which give the concentration of free carriers to the effective mass of samples, increased by increasing the Cd-content within the annealed films of Cd-Zn-Se network.

4.2. Sellmeier parameters

On the other hand, it was found that the index of refraction (n) at low frequencies is subject to the classical dispersion relationship of the single oscillator model as suggested by Sellmeier, which is given as follows [48,50,51]:

$$\frac{(n_o^2-1)}{(n^2-1)} = 1 - \left(\frac{\lambda_o}{\lambda}\right)^2 \tag{14}$$

$$(n^2-1)^{-1} = \frac{1}{(n_o^2-1)} - \frac{1}{(n_o^2-1)\lambda^2}\lambda^2{}_o \tag{15}$$

From the relation between the speed of light and the frequency and wavelength $c = \lambda\nu$ and from the Max Plank's equation of the photon energy, $E = h\nu$, the wavelength can be expressed as follows: $\lambda = hc/h\nu$, thereby Eqn. (15) can be reformulated as follows [46,47]:

$$(n^2-1)^{-1} = \frac{1}{(n_o^2-1)} - \frac{1}{(n_o^2-1)}\lambda^2{}_o\frac{(h\nu)^2}{(hc)^2} \tag{16}$$

Comparing the last Eqn. with Eqn. (9) which was given as:

$$(n^2-1)^{-1} = \frac{E_o^2-(h\upsilon)^2}{E_d E_o} = \frac{E_o}{E_d} - \frac{(h\lambda)^2}{E_d E_o}$$

Therefore, from the comparison, anyone can conclude that:

$$\frac{1}{(\boldsymbol{n_o^2}-1)} = \frac{E_o}{E_d} \text{ and } \frac{1}{(\boldsymbol{n_o^2}-1)}\boldsymbol{\lambda^2_o}\frac{(\boldsymbol{h\nu})^2}{(\boldsymbol{hc})^2} = \frac{(h\lambda)^2}{E_d E_o}$$

Here, $\frac{1}{(\boldsymbol{n_o^2}-1)} = \frac{E_o}{E_d}$ and $\frac{1}{(\boldsymbol{n_o^2}-1)}\frac{\boldsymbol{\lambda^2_o}}{(\boldsymbol{hc})^2} = \frac{1}{E_d E_o}$

Simplifying the last two equations with each other, to get:

$$E_o = \frac{(hc)}{\lambda_o} \,\&\, E_d = (n_o^2-1)\frac{(hc)}{\lambda_o} \,\&\, S_o = \frac{(n_o^2-1)}{\lambda_o{}^2} \tag{17}$$

Hence, substitute by the dispersion energy values of E_o, E_d to get the oscillator wavelength (λ_o) and the strength of the oscillator (S_o). The deduced values of Sellmeier parameters ((λ_o and S_o) have been also listed in Table 3. Furthermore, the values of the previous parameters could also have been inferred from a graphical representation after reformulating Eqn. (14) as follows [6,47]:

$$(n^2-1)^{-1} = \frac{1}{S_o\lambda_o^2} - \frac{1}{S_o\lambda^2} \tag{18}$$

Thus, if anyone draws a graphical relationship between the two variables; the refractive index parameter [$(n^2 - 1)^{-1}$] and the square of the inverse of the wavelength [$(1/\lambda)^2$]; he gets gets a straight line. This line intercepts the vertical axis in a portion of the value ($\boldsymbol{1/S_o\lambda_o^2}$), and its slope is the amount ($\boldsymbol{1/S_o}$). Therefore, the value of the strength of the oscillator, S_o can be determined from the slope, while the value of the wavelength of the oscillator, λ_o can be also calculated from the interception part and the slope. It can observe that the values of (S_o) decreased, when Cd-content increased in the annealed films of $Cd_xZn_{1-x}Se$ network.

4.3. Absorption and extinction coefficients evaluation

If the thickness (d) of the film sample is known, then it is easy to evaluate the absorption coefficient (α) via the knowing of the absorbance (A).

To obtain the absorbance spectra from the transmittance, T-spectra, it can use this equation which was suggested by Connell and Lewis and given as [52]:

$$A = \frac{B + [B^2 + 2qT_a(1 - R_2R_3)]^{1/2}}{q} \tag{19}$$

whereas, B and q are two equations were assumed to relate between the absorbance of the film sample, A and the reflections at (1) the interface of the air-film (R_1), (2) the interface of the film-substrate (R_2) and (3) the interface of the substrate-air (R_3). They can be computed as proposed by Connell and Lewis (1973) using the following set of Eqs. [52]:

$$B = (R_1\text{-}1)(R_2\text{-}1)(R_3\text{-}1) \text{ and } q = 2T_\alpha\,(R_1R_2 - R_1R_3 - R_1R_2R_3)$$

At the same time, the value of the reflections of R_1, R_2 and R_3 are not dependent on the reflectance of the sample, R-spectra, but depends on the values of the refractive indices for both the film sample, (n) and the used substrate (s). The parameter (n) has been already determined in the section 3.2.1 and become known. While the reflectance values of R_1, R_2 and R_3 can be computed from Connell and Lewis Eqs. as follows [52]: $R_1 = [(1 - n)/(1 + n)]^2$, $R_2 = [(n - s)/(n + s)]^2$ and $R_3 = [(s - l)/(s + 1)]^2$.

It is worth mentioning that the authors have employed the software of Origin Lab version 2018 to do the previous calculations.

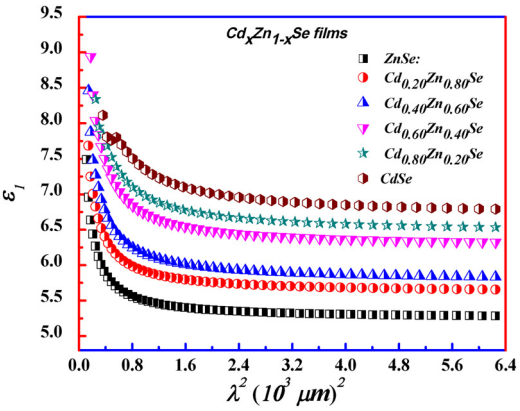

Fig. 9. The variation of the dielectric constant (ε_1) versus (λ^2) for the annealed polycrystalline films of the $Cd_x Zn_{1-x}Se$ matrix, where, ($0.00 \leq x \leq 1.00$).

Since all the previous parameters have been estimated or well known. Thereby, the absorption coefficient (α) can be determined for the film samples of the annealed Cd-Zn-Se matrix, (α) values can be calculated from the following relation [53,54]:

$$\alpha(\lambda) = \frac{1}{t}\ln\left[\frac{(1-R)^2}{2T} + \sqrt{\frac{(1-R)^4}{4T^2} + R^2}\right] \tag{20}$$

Consequently, the estimated (α) values have been graphically represented in Fig. (10) as a function of the incident photon wavelength (λ). It can observe that the absorption coefficient has a large value, of the order about 10^5 cm^{-1}, in the visible region and near the absorption edge, then its value is dramatically decreased after this edge when increasing the wavelength to reach a very low value.

This indicates that after the absorption edge the film become more transparent and the light wave can propagate faster and easier. Moreover, it was found that the absorption edge has shifted towards the higher wavelength, i.e. red shift, with the increasing the ratio of Cd-content, which completely agrees with the previous results of the transmittance, T and the index of refraction, n. These obtained results are in good agreement with the previous literature [1,14,51].

Based on the above, absorption index or the extinction coefficient (k) can now be deduced, where it is directly related to the absorption coefficient (a) by the following Eqn. [47,53]:

$$k = \frac{\alpha\lambda}{4\pi} \tag{21}$$

Fig. (11) illustrates the variation of the absorption index, k with the photon wavelength, λ. As obvious, the k-values are very small tends to zero values after the absorption edge, even before this edge its values were in the order 10^{-2}. This means that the present films become good transparent materials and the absorption of light is minimum in UV and IR-regions.

4.4. Optical band-gap and Urbach energies

The band gap is the space separation between the valence band (VB) and conduction band (CB), thereby the band-gap energy is

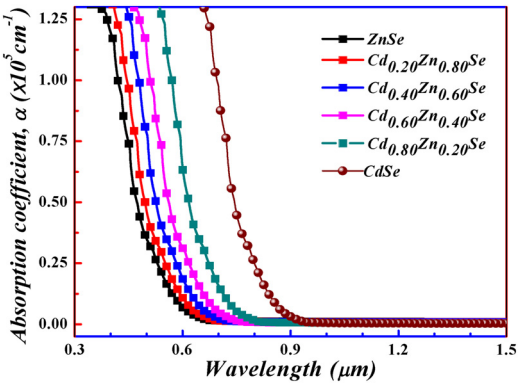

Fig. 10. The dependence of the absorption coefficient (α) upon the wavelength (λ) of the polycrystalline films of the ternary $Cd_x Zn_{1-x}Se$ system, where ($0.00 \leq x \leq 1.00$).

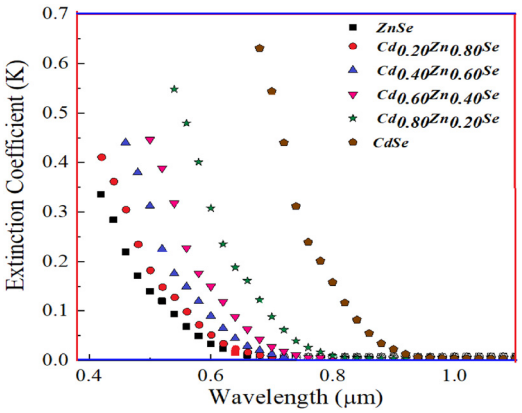

Fig. 11. The graphical relationship between the extinction coefficient, k and the wavelength, λ of the polycrystalline films of the chalcogenide $Cd_x Zn_{1-x}Se$ system, where ($0.00 \leq x \leq 1.0$).

that energy that required for electron to overcome this space and transfer from VB to CB. The value of this energy is very significant to functionalize the semiconducting material in the potential application or the opto-electronic devices. The optical energy gap E_g can be deduced from the absorption coefficient (α) and the energy of photons (hν) using Tauc's formula. This formula can successfully deduce E_g of the semiconducting material in the strong absorption region. It is given as follows [53–55]:

$$\alpha h\nu = \alpha_o (h\nu - E_g)^n \tag{22}$$

where, α_o is some constant called the band-tail parameter and it does not depend on the energy. While E_g is the optical band-gap energy, which is required to get. Along with, the parameter (n) is called the transition mode power factor, its value depends on the type of the electronic transition. For direct and allowed transition, it equals 1/2 and for indirect allowed transition, it is equal 2 [56,57]. But, for the forbidden transitions if they direct and indirect, n equals 3/2 and 3, respectively. Hence, to know the electronic transition type, the person must plot a graph between $(\alpha h\nu)^{1/n}$ and (hν), he will get a straight line, its extrapolation will intercept the horizontal axis (i.e., when $(\alpha h\nu)^2 = 0$) in a point, at which E_g-value is obtained. Taking into consideration that he must plot his graph with compensating about n = (½), 2, 3/2 and 3 and the case that gives the longest straight line would be chosen. In the present case of the annealed film samples of the ternary alloys of Cd-Zn-Se matrix, and after making many trials, it was found that the transition is the direct allowed transition, where n = (1/2) is verified [6,56].

Fig. (12) shows the verification of Equation (22), where it depicts how to get the optical band-gap energy values of the films of the Cd-Zn-Se alloys. The obtained band-gap energy values have been also recorded in Table 3. It can see that E_g-values decrease with increasing the Cd-content in the film samples of the chalcogenide Cd-Zn-Se alloy. Moreover, Fig. (14 -a) exhibits the decreasing of E_g-values as the Cd-content was increased. The relation was best fitted to get the following linear Eq.:

$$E_g \text{ (eV)} = 2.667 - 0.990\ x \tag{23}$$

Where, $0 \leq x \leq 1.0$, it is the ratio of the present Cd-content within the film sample of the Cd-Zn-Se alloys. As obvious from Eqn. (23) that the slope of the equation is negative, which means the decreasing of Eg-values as X increased. As well as, if anyone compensates by x = 0, he can get the optical band-gap energy of the ZnSe sample, but if he compensates by x = 1, he will obtain the optical band-gap energy of the CdSe sample. In addition, the correlate between the optical band-gap energy, E_g and the effective

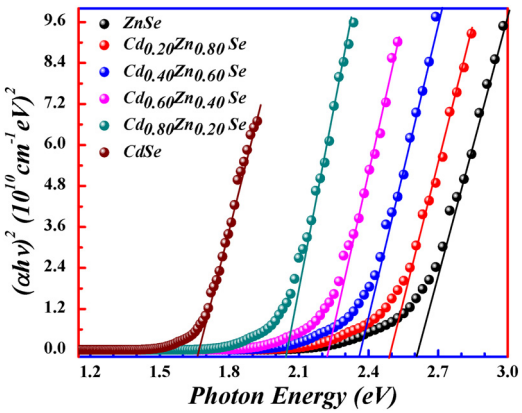

Fig. 12. Determination of the optical band-gap energy, E_g of the polycrystalline films of the chalcogenide $Cd_x Zn_{1-x}Se$ system.

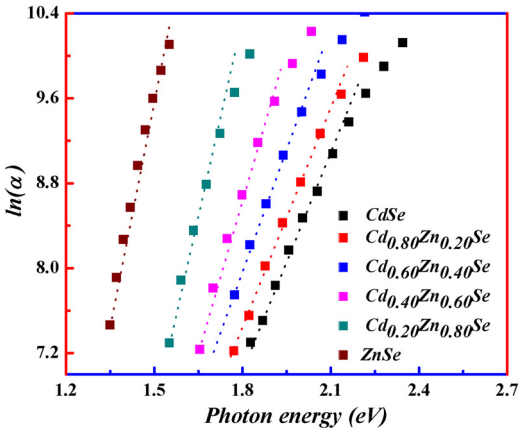

Fig. 13. Evaluation of the band-tail width, E_e of the polycrystalline annealed films of the ternary $Cd_x Zn_{1-x}Se$ system.

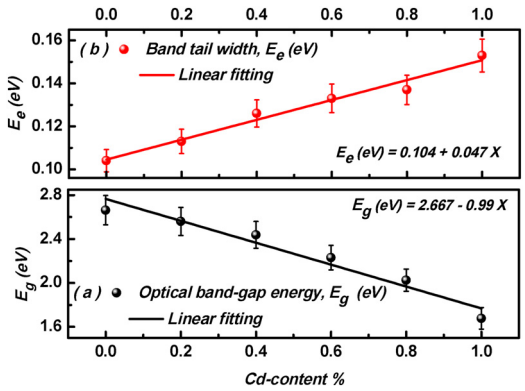

Fig. 14. Dependencee of (a) the band-gap energy, E_g and (b) the energy of the band-tail width, E_e upon the Cd-content percent of the polycrystalline annealed $Cd_x Zn_{1-x}Se$ films.

single oscillator energy E_o can be deduced. It can observe that indeed E_o is equal to about the twice of E_g as suggested by Tanaka [45]. These results affirm on the precision of the calculated values of the obtained parameters. Moreover, the band-tail parameter (α_o) depends on the material type, the optical absorption ability of the material itself and the electronic transition. The values of this parameter have been calculated and tabulated also in Table 3. It is found that the α_o-values of α_o are decreased from 9.152×10^5 cm^{-1} to 4.695×10^5 cm^{-1} with increasing the Cd-content from 0.0 to 1.0. It can also observe that the α_o-values decrease with the decreasing of the band-gap energy value and the increasing of the refractive index values (see Table 3). These results confirm that Cd-ZnSe film samples have semiconductor behavior. As our knowledge, nobody has touched this parameter before and therefore the authors have not been able to find any references can confirm or deny this observation.

On the other hand, near the absorption edge and along the curve of the absorption coefficient, Fig. (10), there is an exponential part is named as "the band-tail width" or "Urbach tail". This exponential part is well evident in the amorphous, the partially crystalline and the disordered semiconducting materials [54,55–58]. Where, these materials are characterized by the presence of localized states extended within the band gap, these localized states lead to decreasing the E_g-values [58–60].

Hence, this tail should be discussed and what so called the energy of the band-tail width or Urbach energy must be evaluated. Urbach suggested an empirical relation could be applied to the curve of absorption coefficient at the low photon-energy region given as [53–58]:

$$\alpha = \beta \exp\left(\frac{h\upsilon}{E_e}\right) or\ \ln\alpha = \ln\beta + \left(\frac{h\upsilon}{E_e}\right) \tag{24}$$

Where, β is some constant and E_e is the energy of the band-tail width. Plotting a graph between (lnα) on the vertical axis and (hν) on the horizontal axis, then anyone can obtain a straight line of slope equals ($1/E_e$) [54,58]. Fig. (13) shows this graphical representation of the Cd-Zn-Se films, hence E_e- values can be obtained and then recorded in Table 3, as well. It is worth to note that the deduced E_e- values are small values and increased from 0.104 eV to 0.153 eV as Cd-content increased. These small E_e-values indicate that the annealed Cd-Zn-se films have reasonable crystallinity and their disordered degree is very low [54,59]. As well as, the addition of more Cd leads to increase the crystallinity nature of films. These results are in good consistent with those obtained by X-ray diffractograms, which exhibits that the crystallite size, D is increased as Cd increased.

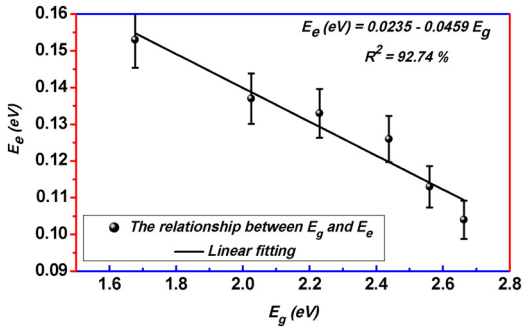

Fig. 15. The interrelationship between E_g and E_e of the polycrystalline annealed films of the ternary $Cd_x Zn_{1-x}Se$ alloys.

Furthermore, the dependence of the band-tail-width energy, E_e upon the Cd-percentage in the film samples of the ternary Cd-Zn-Se system was illustrated also in Fig. (14 -b). The dependence relationship of E_e upon the Cd-ratio was linearly fitted to obtain the following empirical Eq.:

$$E_e \text{ (eV)} = 0.104 + 0.047 \text{ x} \tag{25}$$

where, x is the percentage of the Cd-contained within the film sample, x is ranged between 0 and 1.0. As obvious, the slope of the Eq. (25) is positive, which affirms the increase of E_e-values as x was increased.

Further, if the interrelationship between the optical-band-gap energy and the energy of the band-tail-width is discussed, one can observe that when the Cd-content increased, both of E_g decreases and the band tail energy increase, i.e. there is an inverse proportion between them. This inversely proportional result was illustrated in Fig. (15). The decreasing of E_g is owing to that the addition of the Cd, which leads to decrease the optical energy gap, where it increased on the expense of Zn within the ternary CdZnSe films. On the same time adding more Cd leads to the improvement of the crystallinity and thereby E_e increased, where they have opposite behavior. These changes in both E_g and E_e were analyzed and discussed based on Mott and Davis's model [61]. Where, Mott and Davis postulated that the relation between these two energies is usually inversely proportion for the partial crystalline, disordered and amorphous semiconducting materials [62–64]. For the present case of polycrystalline Cd-Zn-Se, it is inversely proportion relation according to the crystallinity nature of the samples. This is attributed to that increasing of Cd-content improves the crystallinity nature of the films, along with, due to their annealing as mentioned before, too. Where annealing process improves the crystallinity degree of films [3].

As obvious from Fig. (15) that the relation between the two energies (E_g and E_e) has been fitted linearly to obey the following experimental Eq.:

$$E_e \text{ (eV)} = 0.232 - 0.048 \; E_g\text{(eV)} \tag{26}$$

This equation exhibits that there is an inverse proportionality between the band-gap and band-tail width energies for film samples of the CdZnSe system, which is almost verified for the semiconducting materials of polycrystallinity materials, as in the present case [61].

4.5. Cohesive energy and average coordination number

The change in the physical characterization of any material is resulted due to the changes in either bond energies, bond angles or bond lengths. According to the model of the chemical bond approach, CBA any atom of any element of a chemical composition prefers to bond to another atom from another element. Strong bonds firstly are formed before weaker bonds and they form in a descending order according to their strengths [62]. The cohesive energy or the average stabilization energy, CE of any composition is the total sum of the products of the number of probable formed bonds times their energies, hence it can be computed from the following formula [9,62–64]:

$$CE = \sum_i \frac{N_i E_{Bi}}{100} \tag{27}$$

where, N_i is the number of expected formed bonds, E_{Bi} is the energy of that bond. The energy of chemical bonds is classified into two types; homopolar, which is the bond between two similar atoms from the same element and heteropolar, which is the formed bond between two dissimilar atoms and belong to two different elements. Due to the importance of the energy values of homopolar and heteropolar bonds, they had been mentioned in several books [65–67]. So, it is easy to get their energy values. Otherwise, the heteropolar bond energies can be calculated using the following relation [54,62]:

$$B(X-Y) = [B(X-X).\, B(Y-Y)]^{1/2} + 30(\chi_{X-}\chi_Y)^2 \tag{28}$$

where, $\boldsymbol{\chi_X}$ and $\boldsymbol{\chi_Y}$ are the electronegativities of two different atoms (X and Y), which is bonded together. Along with, B(X-X) and B(Y-Y) are the homopolar bond energy values of the two elements X and Y, respectively. Equation (25) has been employed to compute the

values of the cohesive energy, CE for each composition, thereby the obtained values were tabulated in Table 3, too. It is observed that the values of the cohesive energy have decreased from 4.258 eV/atom to 2.772 eV/atom when the Cd-content was increased from 0.00 to 1,00. This is due to that Cd has increased on the account of Zn and at the same time Zn-Se bond is stronger (has higher energy) than Cd-Se bond. Hence, when Cd-content was increased the number of Zn-Se bonds had decreased and the number of Cd-Se bonds had increased, which in turn leads to decrease the cohesive energy values. Furthermore, the optical band-gap energy, E_g is strongly dependent upon the average stabilization energy, CE. Accordingly, and due to the reasons mentioned above the optical band-gap energy values had also decreased from 2.66 eV to 1.67 eV when Cd-content was increased. On the other hand, the average co-ordination number, $< R >$ of any composition can be calculated from the following formula [56,57]:

$$\langle r\rangle = \left(\frac{\alpha N_A + \beta N_B + \gamma N_C}{\alpha+\beta+\gamma}\right) \tag{29}$$

where, α, β and γ are the fractional ratios of Cd, Zn and Se, respectively, within the Cd-Zn-Se alloys and N_A, N_B and N_C are the coordination numbers of Cd, Zn and Se, respectively. Thus, the average coordination number for each combination of the current Cd-Zn-Se alloys can be calculated. As it is clear that the value $< R >$ is a constant value for all combinations, regardless of the fractional proportions of Cd, Zn, and Se, since the elements which have variable ratios Cd and Zn have the same coordination numbers.

4.6. Nonlinear optical studies

The estimated parameters of SEOM-WDD (E_o and E_d) and the generalized Miller's rule in the limit $\nu \rightarrow 0$ have been employed to compute the third-order nonlinear-optical susceptibility, $\chi^{(3)}$ by using this simple form [68–70]:

$$\chi^{(3)}(esu) = \frac{B}{(4\pi)^4}[n_{(0)}^2 - 1]^4 = 6.82 \times 10^{-15}\left(\frac{E_d}{E_o}\right)^4 \tag{30}$$

where, B is some constant equals to 1.7×10^{-10} (esu) and does not depend on either the photon energy or the crystallinity nature of the materials [3,70]. The computed values of this parameter have been listed in Table 3, too. Furthermore, the nonlinear refractive index, n_2 can also be computed if either the static refractive index, n_o or the optical band-gap energy, E_g is known, as expressed by Tichá and Tichý by their empirical equation [63,70,71]:

$$n_2(\text{esu.(eV)}^4) \cong 12\pi \frac{\chi^{(3)}}{n_o} \tag{31}$$

Hence, n_2 values were calculated and reported within Table 3, too. It was observed that both of the two non-linear optical parameters $\chi^{(3)}$ and n_2 increased when Cd-content within the polycrystalline compositions of Cd-Zn-Se alloys was increased. These results are reasonable, where each of the two parameters are dependent upon the energy of band-gap value, E_g, where, they are inversely proportional to the fourth power of E_g. These results are in a good match with the previous literature [70]. Larger values of $\chi^{(3)}$ and n_2 give such films of Cd-ZnSe alloys a special significance in several potential applications, especially in the communications that depends on the high-speed signals and the optical fiber devices [70].

4.7. Plasma frequency estimation

At lower frequencies in the transparency range of semiconductors, where the damping parameter of electron γ, is less than the dielectric constant, ε and the photon frequency, ω, hence the behavior of the real part of the dielectric constant ε_1 with the photon frequency, ω can be controlled according the following form [46,70]:

$$\varepsilon_1 = \varepsilon_\infty - \left(\omega_p^2/\omega^2\right) \tag{32}$$

where, ω_p is the plasma frequency. Thereby and referring to Fig. (9) that illustrates the variation of the dielectric constant (ε_1) versus (λ^2) the extrapolation of the straight line will intercept the vertical axis in the value (ε_∞). While, the plasma frequency (ω_p) of the present samples can be deduced from the slope of the obtained straight line. The deduced values of both (ε_∞) and (ω_p) have been also tabulated in Table 3. Moreover, the deduced ω_p-values can be employed to get also the concentration of free charge carriers to the effective mass, i.e. the term (N/m^*) (to affirm the above obtained results) from the following expression [48,70]:

$$\omega_p = e\left(\frac{N/m^*}{\varepsilon_o \varepsilon_\infty}\right)^{1/2} \tag{33}$$

whereas, e is the electronic charge and ε_o is the free-space electric permittivity. Since, both ω_p- and S_o-values have been already determined before, hence, the value of the term ($N/m*$) can be computed. The obtained results from Eqn. (31) are typically like those obtained before. This confirms the correctness and the accuracy of the current accounts and that were previously computed above. It is worth noticing that the plasma frequency plays an important role in the absorption of photons. When the frequency of the incident photons is in the same order of the plasma frequency, then there is a coupling between the incident photons and the phonons which leads to great absorption of light. This great absorption affects both the refractive index and energy gap values. Hence, when the

plasma and the photon frequencies are equal, then there is an anomalous dispersion of the refractive index in this region of ωp. When the photon energy increased anyone can see that, the value of the refractive index (n) becomes larger as well as the absorption of incident electromagnetic radiation is increased, too. This, in turn, leads to deaccelerating of the propagation of light in the material [48].

4.8. Evaluation of conduction and valence band positions

The VB and CB positions can easily be determined if both the electron affinity, E_{EA}^{M} (eV) and ionization energies, E_{Ion}^{M} (eV) are recognized for any specified material, M. For the present case of the ternary Cd-Zn-Se samples, the position of the conduction band, CB can be estimated from these Eqs. [72–74]:

$$E_{CB}^{0} = E_C - X + \frac{E_g}{2} \tag{34-a}$$

$$\text{Where, } X = \left[\left(X_{Cd}^{x} \times X_{Zn}^{y} \times X_{Se}^{z}\right)^{1/(x+y+z)} \right] \tag{34-b}$$

$$X_{Cd}^{x} = \left(\frac{E_{EA}^{Cd} + E_{Ion}^{Cd}}{2} \right)_{Cd}^{Cd-ratio} \;\&\; X_{Zn}^{y} = \left(\frac{E_{EA}^{Zn} + E_{Ion}^{Zn}}{2} \right)_{Zn}^{Zn-ratio} \text{ and } X_{Se}^{z} = \left(\frac{E_{EA}^{Se} + E_{Ion}^{Se}}{2} \right)_{Se}^{Se-ratio}$$

$$\text{Or for simplicity } X_M = \left(\frac{E_{EA}^{M} + E_{Ion}^{M}}{2} \right)_{M}^{M-ratio} \tag{34-c}$$

Here, the letter M refers to the element (either Cd, Zn or Se) [72–74]. In the above equation, (E_{CB}^{0}) is the potential of CB expressed in eV, E_C is an energy constant for all cases, it is given as $E_C = 4.5$ eV [73], X is a parameter of energy dimensions dependent upon the elemental constituents of the semiconducting composition, while Eg is the determined values of the optical band-gap energy of the film samples of the Cd-Zn-Se solid solutions. Moreover, E_{EA}^{M} gives the energy of electronic affinity of each element, it is equal the difference ($E_{VB} - E_{CB}$) and the ionization energy, E_{Ion}^{M} of each constituent element, M (i.e. refers to Cd, Zn and Se). The electron-affinity value, E_{EA}^{M} and the ionization energy value, E_{Ion}^{M} were listed in Table 4, along with the evaluated X-values of each used elements (Cd, Zn and Se) [72,73].

By knowing these values, the positions of both the conduction and the valence bands (CB and VB, respectively), as well as the CB- and VB-potential values could be calculated for the present samples of Cd-Zn-Se systems. The estimated values were listed also in Table 4 and graphically depicted in Fig. (16). This figure shows that the positions of both CB and VB of $Cd_xZn_{1-x}Se$ solid-solution system have been shifted toward less negative and less positive potentials when the Cd-content was increased within the Cd-Zn-Se system. These results are in good match with the other chalcogenide semiconductor compositions [56,72–75].

4.9. Conclusions

Ternary compositions of $Cd_xZn_{1-x}Se$ matrix (x = 0, 0.2, 0.4, 0.6, 0.8 and 1.0) have been synthesized by using the solid solution reactions method, using elemental powders of Cd, Zn and Se elements of high purity degree (5 N). X-ray diffraction revealed that the thermally evaporated as-deposited films have the amorphous nature and after their annealing, they exhibit the polycrystalline nature of face centered cubic structures. Several optical parameters and characteristics of the annealed film samples have been estimated and studied. Swanepoel's envelope procedures using transmittance and reflectance spectra were utilized to estimate the thickness of films and their complex refractive indices. The Single effective oscillator Model of Wemple Di-Domenico was utilized to evaluate the refractive-index dispersion and some other related parameters like the average energy-gap, E_o and the dispersion-energy, E_d values. Based on the deduced values of both E_o and E_d, the moment values of the optical spectra M_{-1} and M_{-3} have been deduced and investigated. As well as, Sellmeier parameters, which are the oscillator wavelength (λ_o) and the strength of the oscillator (S_o) have also been studied and discussed.

Both the absorption and extinction coefficients were studied and their interrelationship with the Cd-content within the Cd-Zn-Se alloys has been also discussed. The absorption coefficient values were in the order of 10^5 cm^{-1} before the absorption edge of samples, but they dramatically decreased to lower values after this edge for all samples. The optical band-gap and band tail width energies (E_g and E_e) have also estimated by using Tauc and Urbach plots. It was found that E_g and E_e-values have opposite behavior to each other

Table 4
The electronic-affinity energy values, the ionization-energy values of Cd, Zn and Se-elements. In addition, the optical band-gap energy (E_g) and the parameter, X_M-values. Along with, the estimated values of the conduction and valence band positions of film samples of chalcogenide $Cd_xZn_{1-x}Se$ compositions.

Element	E_{EF}^{M} (kJ/mol)	E_{Ion}^{M} (kJ/mol)	X_M (kJ/mol)	Samples of $Cd_xZn_{1-x}Se$ system	E_C (eV)	X-Values (eV)	E_g (eV)	E_{CB}^{0}, CB potential (eV)	E_{VB}^{0}, VB potential (eV)
Cd	0.00	867.8	433.90	ZnSe	4.5	5.266	2.663	- 0.606	2.057
				$Cd_{0.2}Zn_{0.8}Se$		5.241	2.560	- 0.539	2.021
Zn	0.00	906.4	453.20	$Cd_{0.4}Zn_{0.6}Se$		5.220	2.438	- 0.499	1.939
				$Cd_{0.6}Zn_{0.4}Se$		5.197	2.230	- 0.418	1.812
Se	195	940.9	567.95	$Cd_{0.8}Zn_{0.2}Se$		5.174	2.025	- 0.339	1.686
				CdSe		5.146	1.677	- 0.193	1.484

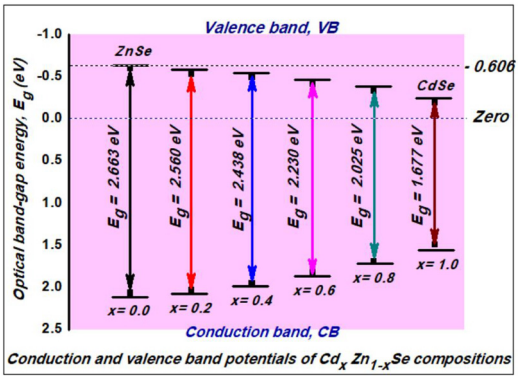

Fig. 16. Valence and conduction band positions of the film samples of $Cd_xZn_{1-x}Se$ compositions, where x = 0.0, 0.2, 0.4, 0.6, 0.8 and 1.0.

with increasing the Cd-ratio within the films. The E_g values decreased from 2.663 to 1.677 eV, while E_e increased from 0.104 to 0.153 eV as Cd-content increased from 0.00 to 1.00.

The chemical bond approach model was also utilized to determine and study the cohesive energy of the ternary chalcogenide compositions of Cd-Zn-Se alloys. It was found that the cohesive energy values decreased from 4.258 to 2.772 eV/atom as the cadmium content increased In addition, the average coordination numbers of all studied compositions were invariant, where Cd and Zn have the numbers of coordination. The interrelationship between CE and E_g were also discussed. Some nonlinear optical parameters have been also evaluated and studied such as the third order nonlinear optical susceptibility and the nonlinear index of refraction. Moreover, the positions of both conduction and valence bands of the ternary $Cd_xZn_{1-x}Se$ samples have been determined. Their positions were shifted toward less negative and less positive potentials when the Cd-content was increased. Finally, it is recommended to employ $Cd_xZn_{1-x}Se$ samples in many applications and devices, especially which dependent on the high-speed signals and the optical fiber devices.

Conflicts of interest

The authors declare that they have no conflict of interest.

This research was not funded by any authority, entity or individual other than the authors themselves. They bear all the costs of the work.

Acknowledgment

The authors gratefully thank the Deanship of Scientific Research at King Khalid University for the financial support through research groups program under grant number (R.G.P.2/34/40).

References

[1] T.C.M. Santhosh, K.V. Bangera, G.K. Shivakumar, J. Alloys and Compounds 703 (2017) 40–44.
[2] Kai Ou, S. Wang, G. Wan, M. Huang, Y. Zhang, L. Bai, Lixin Yi, J. Alloys and Compounds 726 (2017) 707–711.
[3] A.S. Hassanien, K.A. Aly, Alaa A. Akl, J. Alloys and Compounds 685 (2016) 733–742.
[4] G.T. Chavan, S.T. Pawar, V.M. Prakshale, S.M. Pawar, S. Ezugwu, N.B. Chaure, S.S. Kamble, N.N. Maldar, L.P. Deshmuk, Materials Science in Semiconductor Processing 71 (2017) 447–453.
[5] Chien-Hao Huang, Chien-Hsin Yang, Yeong-Tarng Shieh, Tzong-Liu Wang, J. Alloys and Compounds 748 (2018) 265–272.
[6] A.S. Hassanien, Alaa A. Akl, J. Alloys and Compounds 648 (2015) 280–290.
[7] A.S. Hassanien, Alaa A. Akl, Superlattices and Microstructures 85 (2015) 67–81.
[8] S. Selva Priya, B. Lakshmi Shree, P. Therasa Ranjani, P. Karthick, K. Jeyadheepan, M. Sridharan, Materials Today: Proceedings 3 (2016) 1487–1493.
[9] A.S. Hassanien, A.A. Akl, J. Non-Crystalline Solids 428 (2015) 112–120.
[10] A.S. Hassanien, A.A. Akl, J. Non-Crystalline Solids 432 (2016) 471–479.
[11] A.S. Hassanien, A.A. Akl, J. Non-Crystalline Solids 487 (2018) 28–36.
[12] Farzaneh Garousi, Acta Agraria - Agrártudományi Közlemények, GRáRTUDOMányI KöZLEMényEK 64 (2015) 33–38.
[13] A.S. Hassanien, A.A. Akl, CrystEngComm 20 (2018) 7120–7129.
[14] S.R. Deo, A.K. Singh, L. Deshmukh, L.J. Paliwal, R.S. Singh, R. Adhikari, J. Saudi Chemical Society 18 (2014) 327–339.
[15] S.D. Chavhan, S.V. Bagul, R.R. Ahire, N.G. Deshpande, A.A. Sagade, Y.G. Gudage, J. Ramphal Sharma, Alloys and Compounds 436 (2007) 400–406.
[16] V. Korostelin Yu, V.I. Kozlovsky, A.S. Nasibov, P.V. Shapkin, J. Cryst. Growth 159 (1996) 181.
[17] M. Celalettin Baykul, Nilgun Orhan, Thin Solid Films 518 (2010) 1925–1928.
[18] M. Yunus Akaltun, Ali Yıldırım, Aytunc¸ Ates, M. Yıldırım, Materials Research Bulletin 47 (2012) 3390–3396.
[19] B. Schreder, T. Ku¨mmell, G. Bacher, A. Forchel, G. Landwehr, A. Materny, W. Kiefer, J. Cryst. Growth 787 (2000) 214–215.
[20] L. Borkovska, N. Korsunska, V. Kladko, M. Slobodyan, O. Yefanov, Y. Venger, T. Kryshtab, Y. Sadofyev, I. Kazakov, Microelectronics Journal 39 (2008) 589–593.
[21] C. Trager-Cowan, D.M. Bagnall, F. McGow, W. McCallum, K.P. O'Donnell, P.C. Smith, P.J. Wright, B. Cockayne, K.A. Prior, J.T. Mullins, G. Horsburgh, C. Cavenett, J. Crystal Growth 159 (1996) 618–622.
[22] D.R. Rao, R. Islam, Thin Solid Films 224 (1993) 195–199.
[23] R. Islam, D.R. Rao, J. Materials Science Letters 13 (1994) 1637–1639.

[24] K.R. Murali, A. Austine, Chalcogenide Letter 6 (2009) 23–2.
[25] J.E. Williams, R.P. Camata, V.V. Fedorov, S.B. Mirov, Applied Physics A: Materials Science and Processing 91 (2008) 333–335.
[26] R. Venugopal, R.P. Vijayalakshimi, D.R. Reddy, B.K. Reddy, J. Materials Science 31 (1996) 4081.
[27] R. Swanepoel, J. Phys. E 16 (1983) 1214.
[28] Kamal A. Aly, Applied Physics A 99 (2010) 913–919.
[29] A.S. Hassanien, A.A. Akl, Materials Science in Semiconductor Processing 74 (2018) 183–192.
[30] A.S. Hassanien, A.A. Akl, A.H. Saaedi, CrystEngComm 20 (2018) 1716–1730.
[31] A.S. Hassanien, U.T. Khatoon, B. Physica, Condensed Matter 554 (2019) 21–30.
[32] M. Ashraf, S.M.J. Akhtar, A.F. Khan, Z. Ali, A. Qayyum, J. Alloys and Compounds 509 (2011) 2414.
[33] Kai Ou, Shenwei Wang, Liyuan Bai, Kexin Zhang Yu Wang, Lixin Yi, Thin Solid Films 669 (2019) 247–252.
[34] Biljana Pejova, J. Irina Bineva, Materials Science: Materials in Electronics 26 (2015) 4944–4955.
[35] H. Bayramoglu, A. Peksoz, Materials Science in Semiconductor Processing 90 (2019) 13–19.
[36] J.C. Manifacier, J. Gasiot, J.P. Fillard, J. Phys. E 9 (1976) 1002.
[37] A. Dahshan, H.H. Amer, K.A. Aly, J. Phys., D. Appl. Phys. 41 (215401) (2008) 7.
[38] K.A. Aly, H.H. Amer, A. Dahshan, Materials Chemistry and Physics 113 (2009) 690.
[39] A.M. Deo Prakash, M. Aboraia, E.R. Shaaban El-Hagary, K.D. Verma, Ceramics International 42 (2016) 2676.
[40] K.A. Aly, Applied Physics A: Materials Science and Processing 99 (2010) 913.
[41] K.A. Aly, H.H. Hegazy, A. Dahshan, Kh. S. Shaaban, Y. Saddeek, S.R. Alharbi, A.M. Ali, S.A. Amin, Applied Physics A: Materials Science and processing 124 (2018) 868.
[42] A.S. Hassanien, I.M. El Radaf, Physica B 585 (2020) 412110, , https://doi.org/10.1016/j.physb.2020.412110.
[43] M. Didomenico, S.H. Wemple, J. Appl. Phys. 40 (1969) 720.
[44] S.H. Wemple, M. Didomenico, Phys. Rev. B 3 (1971) 1338.
[45] K. Tanaka, Thin Solid Films 66 (3) (1980) 271–279.
[46] A.S. Hassanien, I. Sharma, Optik 200 (2020) 163415.
[47] A.S. Hassanien, A.A. Akl, Physica B 576 (2020) 411718.
[48] A.S. Hassanien, J. Alloys and Compounds 671 (2016) 566–578.
[49] J.N. Zemel, J.D. Jensen, R.B. Schoolar, Physical Review A 140 (1965) 330.
[50] K.A. Aly, F.M. Abdel-Rahim, J. Alloy. Compd. 561 (2013) 284–290.
[51] A.K. Walton, T.S. Moss, Proceedings of the Physical Society 81 (1963) 509.
[52] G.A.N. Connell, A.J. Lewis, Phys. Status Solidi (b) 60 (1973) 291.
[53] A.S. Hassanien, Alaa A. Akl, Applied Physics A: Materials Science and Processing 124 (2018) 752.
[54] A.S. Hassanien, Alaa A. Akl, Superlattices and Microstructures 89 (2016) 153–169.
[55] J. Tauc, Amorphous and Liquid Semiconductors, Plenum, New York, 1974.
[56] A.S. Hassanien, I. Sharma, J. Alloys and Compounds 798 (2019) 750–763.
[57] A.S. Hassanien, I. Sharma, A.A. Akl, J. Non-Crystalline Solids 531 (2020) 119853.
[58] F. Urbach, Physical Review 92 (1953) 1324.
[59] S.J. Ikhmayies, R.N. Ahmad-Bitar, Proceedings of the Eleventh World Renewable Energy Congress and Exhibition, (2010), p. 979.
[60] L.L. Kazmersky (Ed.), Polycrystalline and Amorphous Thin Films and Devices, Academic Press, New York, 1980, p. 135.
[61] N.F. Mott, E.A. Davis, Electronic processes in non-crystalline materials, Clarendon Press, Oxford, 1979.
[62] J. Bicerano, S.R. Ovshinsky, J. Non-Cryst. Solids 74 (1985) 75.
[63] I.M. El Radaf, H.Y.S Al-Zahrani, A.S. Hassanien, J. Mater. Sci., xxx (2020) xxx, https://doi.org/10.1007/s10854-020-03369-9.
[64] A. Dahshan, K.A. Aly, J. Non-Crystalline Solids 408 (2015) 62.
[65] L. Pauling, The Nature of the Chemical Bond, 3rd Edition, Cornell University Press, Ithaca, NY, 1960.
[66] Y.R. Luo, Comprehensive Handbook of Chemical Bond Energies, CRC Press, Boca Raton, FL, 2007.
[67] David R. Lide (Ed.), CRC Handbook of Chemistry and Physics, 88th edition, Taylor & Francis Group, Boca Raton, Florida, 2008.
[68] C.C. Wang, Phys. Rev. B 2 (6) (1970) 2045.
[69] J.J. Wynne, Phys. Rev. 178 (1969) 1295.
[70] K.A. Aly, Y. Saddeek, Gh Abbady, S.R. Alharbi, J. Non-Crystalline Solids 475 (2017) 161–166.
[71] H. Tichá, L. Tichý, J. Opt. Adv. Mater. 4 (2) (2002) 381.
[72] C. Xing, Y. Zhang, W. Yan, L. Guo, Int. J. Hydrogen Energy 31 (2006) 2018.
[73] M. Askari, N. Soltani, E. Saion, W.M. Mat Yunus, H.M. Erfani, M. Dorostkar, Superlattices Microstruct. 81 (2015) 193.
[74] Rui Xie, Jinzhan Su, Ya Liu, Liejin Guo, Int. J. Hydrogen Energy 39 (2014) 3517.
[75] Zhen Liu, Jingjing Zhang, Yang Lv, Xin Zhou, Shenmin Li, J. Alloys and Compounds 700 (2017) 1–11.